Molecular Biology of the Cell
Vol. 9, 2681–2697, September 1998

Coupled Translocation Events Generate Topological Heterogeneity at the Endoplasmic Reticulum Membrane

Kenneth Moss, Andrew Helm, Yun Lu, Alvina Bragin, and William R. Skach*

Departments of Molecular and Cellular Engineering and Medicine, University of Pennsylvania, Philadelphia, PA 19104

Submitted January 13, 1998; Accepted June 10, 1998
Monitoring Editor: Peter Walter

Topogenic determinants that direct protein topology at the endoplasmic reticulum membrane usually function with high fidelity to establish a uniform topological orientation for any given polypeptide. Here we show, however, that through the coupling of sequential translocation events, native topogenic determinants are capable of generating two alternate transmembrane structures at the endoplasmic reticulum membrane. Using defined chimeric and epitope-tagged full-length proteins, we found that topogenic activities of two C-*trans* (type II) signal anchor sequences, encoded within the seventh and eighth transmembrane (TM) segments of human P-glycoprotein were directly coupled by an inefficient stop transfer (ST) sequence (TM7b) contained within the C-terminus half of TM7. Remarkably, these activities enabled TM7 to achieve both a single- and a double-spanning TM topology with nearly equal efficiency. In addition, ST and C-*trans* signal anchor activities encoded by TM8 were tightly linked to the weak ST activity, and hence topological fate, of TM7b. This interaction enabled TM8 to span the membrane in either a type I or a type II orientation. Pleiotropic structural features contributing to this unusual topogenic behavior included 1) a short, flexible peptide loop connecting TM7a and TM7b, 2) hydrophobic residues within TM7b, and 3) hydrophilic residues between TM7b and TM8.

INTRODUCTION

Transmembrane (TM)[1] topology of most eukaryotic integral membrane proteins is established at the endoplasmic reticulum (ER) membrane as specific topogenic determinants (e.g., signal, stop transfer [ST], and signal anchor sequences) emerge from the ribosome and engage their cognate cytosolic and/or membrane bound receptors (Blobel, 1980). This process of topogenesis involves at least four distinct steps: 1) ER membrane targeting, 2) translocation initiation, 3) translocation termination, and 4) membrane integration (reviewed in Rapoport *et al.*, 1996; Johnson, 1997). Topogenic determinants in naturally occurring proteins usually direct these events efficiently and completely, thus ensuring a single uniform topology for any given cohort of nascent polypeptide chains. Failure to complete one or more of these steps, however, may result in proteins with heterogeneous topological outcomes. For example, mutagenesis studies of ST (Kuroiwa *et al.*, 1991) and signal anchor (Parks *et al.*, 1989; Parks and Lamb, 1991) sequences have shown that under certain conditions, topogenic determinants may generate mixed populations of nascent chains exhibiting secretory, N-*trans* (type I) and/or C-*trans* (type II) TM topology. Specialized topogenic determinants in naturally occurring proteins may also direct alternate topologies. In the case of murine plasminogen activator inhibitor 2, cytosolic and secretory iso-

* Corresponding author. Present address: Division of Molecular Medicine, Oregon Health Sciences University, Portland, OR 97201-3098.

[1] Abbreviations used: ER, endoplasmic reticulum; MDR1-Pgp, human P-glycoprotein; Pgp, P-glycoprotein; PK, proteinase K; ST, stop transfer; TM, transmembrane; XO, *Xenopus* oocyte.

forms are generated by a bipartite signal sequence that targets the nascent chain to the ER membrane but initiates translocation for only a fraction of targeted chains (Belin *et al*., 1989, 1996). Similarly, secretory and TM conformations of the prion protein (Hay *et al*., 1987a,b) PrP are directed by a specialized pause transfer sequence that transiently terminates translocation and allows a downstream hydrophobic segment to span the membrane in a subset of nascent chains (Yost *et al*., 1990; Nakahara *et al*., 1994). This TM isoform has been recently linked to pathogenesis of the neurodegenerative prion diseases (Hegde *et al*., 1998). In addition, the topological fate of both plasminogen activator inhibitor 2 and PrP is controlled by cellular factor(s) (Wohlwend *et al*., 1987; Lopez *et al*., 1990), suggesting that such specialized topogenic determinants might provide a mechanism for topological regulation.

Topogenic determinants also direct the topology of multispanning (polytopic) proteins (Friedlander and Blobel, 1985; Audigier *et al*., 1987). In the simplest case, this process proceeds cotranslationally at the ER membrane as independent signal (anchor) and ST sequences direct sequential rounds of translocation initiation, translocation termination, and membrane integration (Rothman *et al*., 1988; Wessels and Spiess, 1988; Lipp *et al*., 1989; Shi *et al*., 1995). Alternatively, native polytopic proteins may acquire their topology through cooperative and/or synergistic interactions between multiple topogenic determinants (Calamia and Manoil, 1992; Skach and Lingappa, 1993; Wilkinson *et al*., 1996; Lu *et al*., 1997). This latter process involves transient uncoupling of translocation and membrane integration events (Skach and Lingappa, 1993; Lin and Addison, 1995), posttranslational translocation of peptide loops (Lu *et al*., 1997), or even posttranslational reorientation of TM helices (Wilkinson *et al*., 1996). Thus recent studies have added new complexities to the traditional view of polytopic protein biogenesis by demonstrating that a given TM topology may be generated through several alternate combinations of topogenic events.

Because polytopic topology is specified solely by topogenic information encoded within the nascent chain, conflicting or ambiguous topogenic determinants within a single polypeptide may generate proteins in which TM helices are either left out of the membrane or span the membrane in multiple orientations. This phenomenon was recently demonstrated using experimentally engineered polytopic *Escherichia coli* proteins and has been referred to as "topologic frustration" (Gafvelin and von Heijne, 1994). How and whether "topologic frustration" occurs in native polytopic proteins is less clear. The four-spanning protein ductin has been shown to acquire two opposite TM orientations when expressed in vitro in the presence of canine pancreas microsomal membranes (Dunlop *et al*., 1995). Alternate TM topologies have also been reported for several members of the P-glycoprotein (Pgp) family of ABC transporters in whole-cell as well as cell-free expression systems. In this latter case, antibody mapping, cysteine labeling, and epitope insertion studies of functional Pgp at the plasma membrane of mammalian cells (Yoshimura *et al*., 1989; Georges *et al*., 1993; Schinkel *et al*., 1993; Loo and Clarke, 1995; Kast *et al*., 1996) have supported a conventional 12-spanning topology predicted by initial hydropathy analyses (Chen *et al*., 1986; Gros *et al*., 1986). In contrast, other studies of full-length, truncated, and chimeric Pgps expressed in mammalian, cell-free, *Xenopus* oocyte (XO) and prokaryotic expression systems (Zhang and Ling, 1991; Zhang *et al*., 1996; Skach *et al*., 1993; Beja and Bibi, 1995; Poloni *et al*., 1995) have found that a predicted cytosolic peptide loop between TM segments 8 and 9 appears to reside in an extracytosolic location. Moreover, at the ER membrane, this TM8–9 loop appears to be extracytosolic in only a subpopulation (40–50%) of chains, suggesting that in certain cellular compartments Pgp might be capable of achieving both conventional as well as unconventional topologies (Skach *et al*., 1993).

Topological studies of native polytopic proteins raise fundamental questions regarding polytopic protein biogenesis; namely, how does the dynamic behavior of topogenic information encoded within a nascent polypeptide function to generate complex topology at the ER membrane, and what are the limits of variation that govern this behavior in native substrates? Understanding these questions will be critical in defining different mechanisms of polytopic protein assembly, in predicting topological outcome, and ultimately in understanding structure–function relationships of polytopic membrane proteins. In the current study, we address these issues by characterizing functional properties of topogenic determinants encoded within a specific region (TM7 and TM8) of the C-terminal hydrophobic domain of human Pgp (MDR1-Pgp), a region where conflicting topologies have been previously reported. Two determinants, a signal (anchor) sequence (TM7a) and an inefficient ST sequence (TM7b), were identified within an unusually long hydrophobic segment predicted to encompass TM7, whereas a third determinant exhibiting both ST and C-*trans* (type II) signal anchor activity was encoded within TM8. The topogenic events directed by these determinants were directly coupled to generate two different populations of TM chains in the ER membrane with nearly equal efficiency. During this process, TM7 achieved both single- and double-spanning topology, whereas TM8 exhibited both type II and type I topology. The cooperative behavior of these native topogenic determinants provides a novel mechanism by which alternate polytopic TM conformations may be generated in the ER membrane through a

Table 1. TM plasmids

Plasmid	Antisense primer	C-terminus Pgp Fusion site
TM7a.P (I719)	(2) CAGGCCGGTCACCATAATGGCACAAAATAC	I719
TM7a.P (G722)	(3) TGGTTGGGTCACCCCATTTATAATGGCACA	G722
TM7a.P (P726)	(4) TATTGCGGTCACCGGTTGCAGGCCTCCATT	P726
TM7a.P (A729)	(5) TGAAAAGGTCACCGCAAATCGTGGTTGCAG	A729
TM7a/b.P	(6) CAAGTTGGTCACCTGTCGTTTTGTTTCAGGATC	Q750
TM7a/b-8.P	(7) CATTGGTCACCCTGGTAGTCAATGCTCCAGT	R817

series of definable translocation events. We refer to this phenomenon as topological heterogeneity and propose that this process may play a physiological role during the topogenesis of certain native polytopic proteins.

MATERIALS AND METHODS

Construction of cDNA Vectors

Plasmids encoding TM7a through TM8 were generated by PCR amplification of human MDR1 cDNA (Chen *et al.*, 1986) using a sense oligonucleotide encoding an *Nco*I site MDR1-Pgp at bp 1950 (primer 1, GATGCCATGGAAATGTCTTACCCT) and antisense oligonucleotides indicated above (Table 1). Pertinent MDR1 sequence included in these constructs and the location of fusion sites for these and other constructs are indicated in Figure 1.

After 10 cycles of PCR, fragments were digested with *Nco*I and *Bst*EII, gel purified and ligated into an *Nco*I–*Bst*EII-digested, phosphatased vector, S.L.ST.gG.P (Skach and Lingappa, 1993). This generated a series of plasmids encoding a common ATG start codon at MDR1-Pgp residue L650, followed by MDR1-Pgp coding sequence through the C-terminal fusion sites (e.g., MDR1-Pgp codons) listed above, followed by the coding sequence of a previously described P reporter derived from bovine prolactin (Rothman *et al.*, 1988). Plasmids TM8.P and TM2.P were similarly generated using sense and antisense primers (TATTTCCATGGTTATAGGGGTTTTTACA and primer 7 for TM8.P; and sense primer AACTTTTTTAAGGTGACCAATAAAAGTGAAAAAGATAAG and antisense primer CCCAACATCGGTCACCTCAAACCAGCCTATCTCCTGTCG for TM2.P). The amplified coding sequence for TM8 was digested with *Nco*I and *Bst*EII and ligated into S.L.ST.gG.P as described above. The coding

Figure 1. Amino acid sequence of MDR1-Pgp from residue K702 through E782. Residues predicted to constitute potential TM segments 7a, 7b, and 8 are outlined. Pertinent residues and fusion sites for specific plasmids are included, although N-terminal and some C-terminal flanking sequences are left out for clarity. P represents the C-terminal translocation reporter derived from bovine prolactin. Dashed areas represent deleted amino acid residues. Mutated residues are boxed; inserted residues are underlined. Outlined residues represent putative TM domains, and bold residues represent intervening sequences. Residues NFKLLSHCLLVT (plasmids S.gG.X.P) are contributed by the gG reporter domain.

Table 2. S.gG.TM plasmids

Plasmid	Sense	Antisense	MDR1 sequence
S.gG.TM7b.P	(8) ATTATGGTGACCGGCCTGCAACCAGCATT	6	G723-Q750
S.gG.TM7b*.P	(9) AGGCCTGGTGACCGCATTTGCAATAATATT	6	A727-Q750
S.gG.TM7b-8.P	8	7	G723-R817
S.gG.TM7b*-8.P	9	7	A727-R817
S.gG.TM8.P (residues L736-R817)	(10) CAAAGGTGACCGGGGTTTTTACAAGAATTG	7	G737-R817

sequence for TM2 was digested with *Eco*RV and *Bst*EII and ligated into the S.L.ST.gG.P vector digested sequentially with *Nco*I, Klenow fragment, and *Bst*EII. The resultant plasmids thus encode MDR1-Pgp residues I736-R817 (TM8) or I98-F163 (TM2), upstream of the P reporter. Plasmids encoding MDR1-Pgp fragments in the chimera S.gG.-X-.P were generated by digesting PCR-amplified MDR-Pgp cDNA (oligonucleotides indicated below) with *Bst*EII and ligating these fragments into *Bst*EII-digested vector S.gG.P (Rothman *et al*., 1988) (Table 2).

To generate epitope-tagged MDR1-Pgp, a unique *Sac*I site was engineered at codons G812 and A813 using the primer (11) CTGGTAGTCAGAGCTCCAGTGGTGTTTTTAGG and a single-stranded (M13) template (Muta-gene method [Bio-Rad Laboratories, Hercules, CA] described previously; Xiong *et al*., 1997) plasmid pSPMDR1-Sac. We then used the PCR overlap extension method to introduced mutations D743R/D744R. Sense (ATTAGGAGGCCCGAGACAAAACGACAGAATAG) and corresponding antisense oligonucleotides were used together with 5′ primer (1) and 3′ primer (7) as described (Ho *et al*., 1989). The resulting PCR fragment encoding bp 1940–2450 was digested with *Hin*dIII–*Sac*I and ligated into *Hin*dIII–*Sac*I-digested pSPMDR1-Sac to generate pSPMDR1(DD/RR). Plasmids S.gG.TM7b(DD/RR).P and S.gG.TM7b-8(DD/RR).P were generated as described for WT sequences except that the mutant pSPMDR1(DD/RR) was used as template for PCR reactions. Plasmid TM7a/b.P (ΔNGGLQP) was derived by ligating a *Bst*EII fragment from S.gG.TM7b*.P into *Bst*EII-digested TM7a.P (I719). This fusion replaced codons I720-P726 of MDR1 with DNA encoding residues MVT (see Figure 1). This fusion site encoding the (ΔNGGLQP) mutation was identical in subsequent plasmids TM7a/b-8.P (ΔNGGLQP) and full-length MDR1 ΔNGGLQP, which were generated by serial subcloning. WT and mutant plasmids encoding the C-terminal half of MDR1-Pgp were generated by deleting residues M1-A649. Translation of resulting plasmids was initiated at a methionine residue engineered at position L650.

Plasmid pSPMDR1-P was generated by engineering a *Sac*I restriction site at codon 229 of bovine prolactin (via PCR) in the plasmid TM1–8.P (described in Skach *et al*., 1993) and ligating a *Hin*dIII–*Sac*I fragment from this plasmid into *Hin*dIII–*Sac*I-digested pSPMDR1-Sac. The resultant construct encoded the 142 residue P reporter inserted into full-length MDR1-Pgp at codons 817 and 814. D743R/D744R and ΔNGGLQP mutations were subsequently engineered into pSPMDR1-P by ligating *Hin*dIII–*Bst*EII fragments from plasmids TM7a/b-8(DD/RR).P and TM7a/b-8.P (ΔNGGLQP), respectively, into *Hin*dIII–*Bst*EII-digested pSPMDR1-P. Finally, residues encoding TM7b and its C-terminal flanking sequences were deleted from plasmid pSPMDR1-P by introducing *Bst*EII restriction sites at codons 734 and 752 of MDR1 using PCR (antisense oligonucleotide CCCTATGGTCACCGAAAATATTATTGCAAATGCT and sense oligonucleotide 10) and ligating these *Bst*EII sites together. This substituted residues Val-Thr for MDR1 residues I735-S756.

All PCR-amplified or Mutated cDNA Fragments Used for Subcloning Were Verified by Direct Sequencing

Transcription and Xenopus laevis Oocyte Expression

mRNA was transcribed in vitro with SP6 RNA polymerase (New England Biolabs, Beverly, MA) using 2–4 μg of plasmid DNA in a 10-μl volume at 40°C for 1 h as previously described (Rothman *et al*., 1988); 0.5 μl of a 10× concentrated *trans*-^{35}S label (ICN Pharmaceuticals, Irvine, CA) were added to 2 μl of transcription mixture and injected into stage VI XOs (50 nl/oocyte). After incubation at 18°C for 3–4 h, oocytes were homogenized on ice in 10 vol of homogenization buffer (0.25 M sucrose, 50 mM KAc, 5 mM $MgAc_2$, 1.0 mM DTT, 50 mM Tris, pH 7.5) using a hand-held homogenizer in a 1.5-ml Eppendorf tube. Before proteolysis, $CaCl_2$ was added to 10 mM final concentration.

Protease Digestion

Proteinase K (PK) was added to aliquots of XO homogenate (0.2 mg/ml final concentration) in the presence or absence of 1% Triton X-100 and incubated on ice for 1 h. Residual protease was inactivated by rapid mixing with PMSF (10 mM) in 10× vol of 1% SDS, 0.1 M Tris, pH 8.0 (preheated to 100°C). For plasmids expressing full-length and C-terminal halves of MDR1-Pgp, samples lacking PK were not heated to avoid aggregation. Samples were then diluted in 10 vol of Buffer A (0.1 M NaCl, 1% Triton X-100, 2 mM EDTA, 0.1 mM PMSF, and 0.1 M Tris, pH 8.0). Samples were incubated at 4°C for 1–2 h and clarified by centrifugation at 16,000× *g* for 15 min, and supernatants were used for subsequent immunoprecipitation.

Carbonate Extraction

XO homogenates were diluted 300-fold in either sodium carbonate (0.1 M Na_2CO_3, pH 11.5) or Tris (0.25 M sucrose, 0.1 M Tris, pH 7.0) solutions. Freshly synthesized known secretory (bovine prolactin) and TM (S.L.ST.gG.P; Skach and Lingappa, 1993) control proteins were added to each tube before processing. Carbonate solutions were adjusted to pH 11.5 if necessary by addition of small amounts of NaOH. Samples were incubated on ice for 30 min before centrifugation at 70,000 rpm (TLA 100.2 rotor, Beckman, Fullerton, CA) for 30 min. Supernatants were removed, and proteins were precipitated in 20% trichloroacetic acid before washing in acetone and resuspending in 1% SDS and 0.1 M Tris (pH 8.0). Membrane pellets were dissolved directly in 1% SDS and 0.1 M Tris (pH 8.0). Samples were immunoprecipitated before analysis by SDS-PAGE.

Immunoprecipitation and Autoradiography

Oocyte homogenate supernatants were immunoprecipitated by addition of anti-prolactin (ICN Biomedicals, Costa Mesa, CA) or anti-globin (De Fea *et al*., 1994) antisera to a working dilution of 1:1000. After a 10- to 30-min preincubation, 5 μl of protein A-Affigel (Bio-Rad, Hercules, CA) were added, and the sample was continuously mixed at 4°C for 2–10 h before washing three times with Buffer A and twice with 0.1 M NaCl and 0.1 M Tris (pH 8.0). Samples were analyzed by SDS-PAGE, EN^{3}HANCE (New England Nuclear, Boston, MA) fluorography, and autoradiography as described. Autoradiograms were digitized with an AGFA (Mortsel, Belgium) Studio Scan II, and, where indicated, band intensities were quantified on unmodified images using Adobe Systems (Mountain View, CA) Photoshop software.

RESULTS

Initial topological studies of human and rodent Pgps have indicated that predicted cytosolic residues flanking the C terminus of TM8 reside in the ER lumen in ~50% of newly synthesized chains (Zhang and Ling, 1991; Skach *et al.*, 1993). Consistent with these observations, Beja and Bibi (1995) noted that when expressed in *E. coli* as a series of PhoA fusion proteins, murine Pgp TM7 exhibited the capacity to span the membrane twice, and TM8 C-terminal flanking residues resided in the periplasm. Thus they proposed that C-terminal topology of Pgp resembled the corresponding region of a related ABC transporter MalG. In each of these studies, however, the experimentally derived Pgp topology differed from the conventional 12-spanning hydropathy-based model, which has been supported by antibody mapping, epitope insertion, and cysteine labeling studies. To better understand the mechanism by which topology of this peptide region is established, we have identified topogenic determinants encoded within TM7 and TM8 from human MDR1-Pgp and characterized their ability, both independently and together, to direct specific translocation events at the ER membrane.

TM7 Encodes Two Distinct Topogenic Determinants

Like the corresponding regions of MalG and murine Pgp, TM7 from human MDR1-Pgp comprises an unusually long, 38-residue, sequence containing two distinct hydrophobic regions (subsequently referred to as TM7a and TM7b) connected by a short, flexible peptide segment (Figure 2A). We reasoned that if TM7 were able to form two TM segments, then it might encode two distinct topogenic determinants capable of first initiating, and subsequently terminating, nascent chain translocation. TM7a signal sequence activity was therefore tested using a series of plasmids in which TM7a was engineered upstream of a previously defined prolactin-derived translocation reporter, P (Figures 1 and 2A). Constructs were expressed in microinjected XOs, and topology of newly synthesized chains was determined by digesting oocyte homogenates with PK. Under these conditions, the ER-derived microsomal membranes form sealed, right-side-out vesicles (Rothman *et al.*, 1988; Skach and Lingappa, 1994) and translocated reporter domains are protected from digestion in the absence but not the presence of nondenaturing detergent. The uniform sidedness of these vesicle preparations is demonstrated in Figure 2B, where 100% of the secretory protein prolactin was fully protected after protease digestion (lanes 1–30). Likewise, PK digestion of the chimeric type I TM protein S.gG.ST.P resulted in >95% digestion of the P reporter and protection of the N-terminal globin-derived passenger domain (Figure 2B, lanes 4–9).

As shown in Figure 2C, >90% of newly synthesized polypeptides from plasmid TM7a(I719).P generated protease-protected, P-reactive fragments, confirming that TM7a functioned as an efficient signal sequence to translocate C-terminal flanking residues (lanes 1–3). However, when additional C-terminal residues were included along with TM7a (Figure 2C, lanes 4–12), a progressive decrease in the fraction of reporter translocation was observed, indicating that the P reporter was increasingly oriented toward the cytosol. Some chains from plasmid TM7(I719).P adopted a type II TM topology. This was indicated by the appearance of a new, PK-protected 20-kDa P-reactive fragment after PK digestion (Figure 2C, lane 2, double arrow). In addition, a minor fraction (<10%) of chains from each of these constructs appeared to be completely protected from digestion, (i.e., fully secretory). Most chains, however, were cleaved during translocation into the ER lumen, presumably by signal peptidase, generating a 15-kDa fragment consistent with the predicted size of the P reporter (142 residues) (Figure 2C, lanes 2, 5, 8, and 11, upward arrows). This cleavage event was similar to previous studies that demonstrated that removal of downstream TM segments may unmask cryptic signal peptidase recognition sites in otherwise uncleaved internal signal anchor sequences (Schmid and Spiess, 1988; Akiyama *et al.*, 1990; Skach and Lingappa, 1993, 1994; Skach *et al.*, 1994). In addition, signal peptidase cleavage was less efficient in longer constructs, indicating decreased accessibility to the cleavage site. The interpretation that longer chains might exhibit a double-spanning topology was further supported, because uncleaved chains remained membrane associated as determined by pelleting experiments (our unpublished observations).

We next tested whether TM7b functioned independently as an ST sequence by engineering TM7b (residues G723-R749) into the chimeric protein S.gG.P (Figure 2D). In this construct, translocation is initiated by the N-terminal signal sequence (Rothman *et al.*, 1988). An ST sequence located between the gG (globin-derived) and P passenger domains will terminate translocation and direct the otherwise secretory chains into a type I TM topology with N terminus (gG) in the ER lumen and C terminus (P) in the cytosol (Figure 2B) (Rothman *et al.*, 1988; Skach and Lingappa, 1994). As shown in Figure 2D, full-length S.gG.TM7b.P chains (30-kDa bands) and N-linked glycosylated chains (33-kDa bands, downward arrows) were immunoprecipitated with both globin and prolactin antisera before PK digestion (lanes 1 and 4). The relative degree of glycosylation varied somewhat between experiments but did not significantly influence translocation efficiency (our unpublished observations). Forty-one percent of chains exhibited a type I TM orientation, as evi-

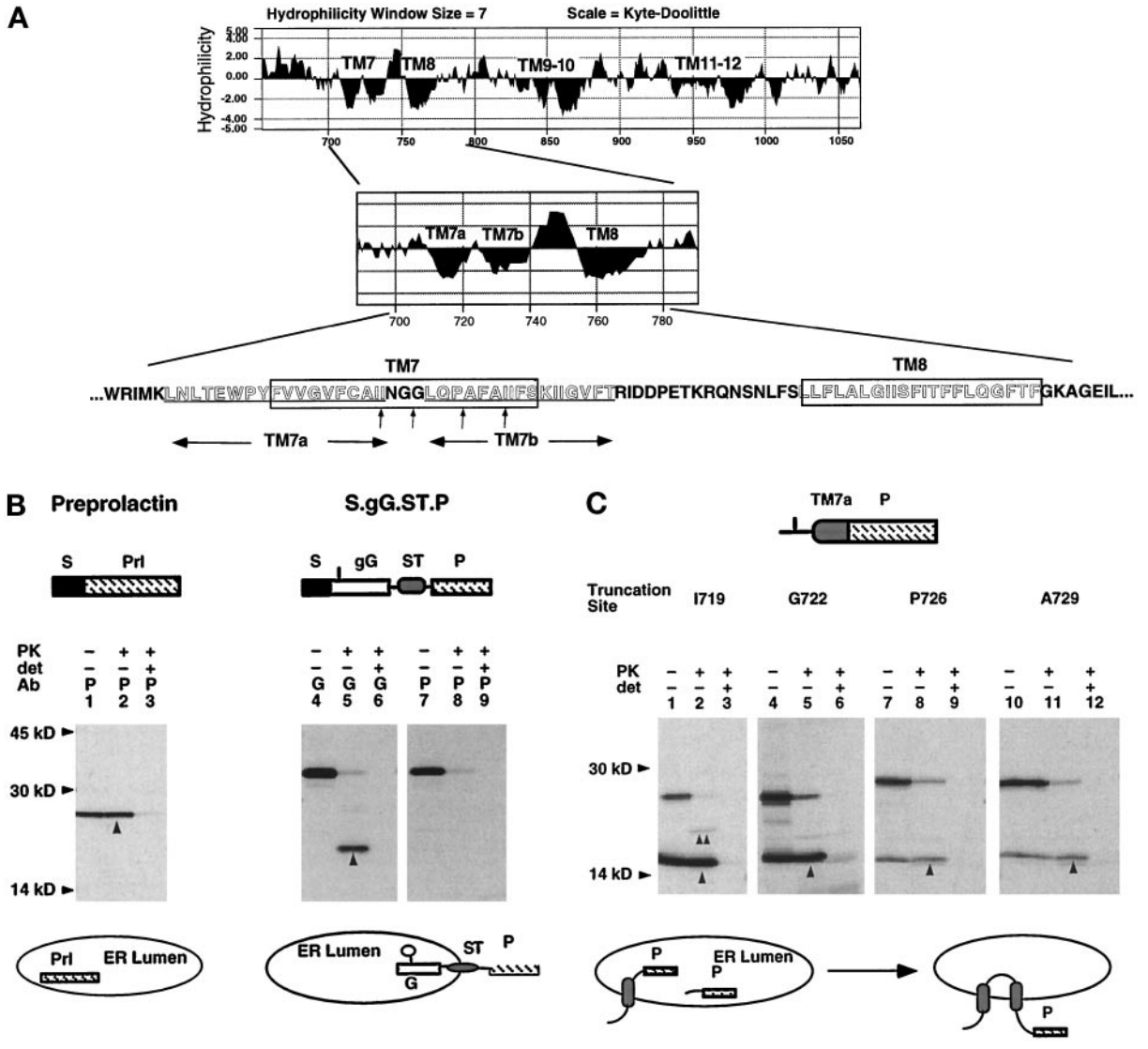

Figure 2. Signal and ST activities of TM7a and TM7b. (A) Kyte–Doolittle hydropathy profile of the C-terminal MDR1-Pgp hydrophobic domain. Location and sequence of potential TM segments are indicated. (B) Mature XOs expressing bovine prolactin (lanes 1–3) and the TM protein S.gG.ST.P (Skach and Lingappa, 1994) (lanes 4–9) were homogenized and digested with PK in the presence and absence of detergent (det), immunoprecipitated with antiprolactin (P) or antiglobin (G) antisera, and analyzed by SDS-PAGE. Upward arrows indicate polypeptides protected from PK digestion. Topology of chains is diagrammed below the autoradiogram. The glycosylation site is indicated in the gG reporter as a vertical line. (C) Plasmids encoding TM7a fused to the P reporter at indicated residues (A, vertical arrows) were expressed in oocytes and analyzed as in B. Upward arrows (lanes 2, 5, 8, and 11) indicate chains protected from protease digestion. Topology of chains is indicated below the autoradiogram to reflect that most uncleaved chains (60–80%) pellet with membranes at neutral pH (our unpublished observations). (D) Plasmid S.gG.TM7b.P was expressed in oocytes and analyzed as in B. Downward arrows indicate full-length, PK-protected glycosylated chains (lanes 2 and 5). Upward arrow (lane 2) indicates the PK protected globin-reactive fragment. For carbonate extraction (lanes 7–10), oocyte homogenates containing S.gG.TM7b.P and TM (S.L.ST.gG.P; Skach and Lingappa, 1993) and secretory (bovine prolactin; Skach and Lingappa, 1993) control proteins were incubated in neutral buffer (Tris) or 0.1 M Na carbonate (Carb) as described in MATERIALS AND METHODS. Supernatants (S) and pellets (P) were immunoprecipitated with prolactin antisera. Topology of chains is indicated.

denced by their accessibility to protease (Figure 2D, lanes 2 and 5, downward arrows) and the appearance of a new, 17-kDa globin-reactive fragment recovered in the absence of detergent (Figure 2D, lane 2, upward arrow). However, slightly more than half of full-length chains (59%) were fully protected from PK digestion, suggesting that these chains were completely translocated into the ER lumen. The secretory nature of these chains was further confirmed by extraction from membranes in 0.1 M sodium carbonate (pH 11.5) (Figure 2D, lanes 7–10). Thus TM7b was capable of terminating transloca-

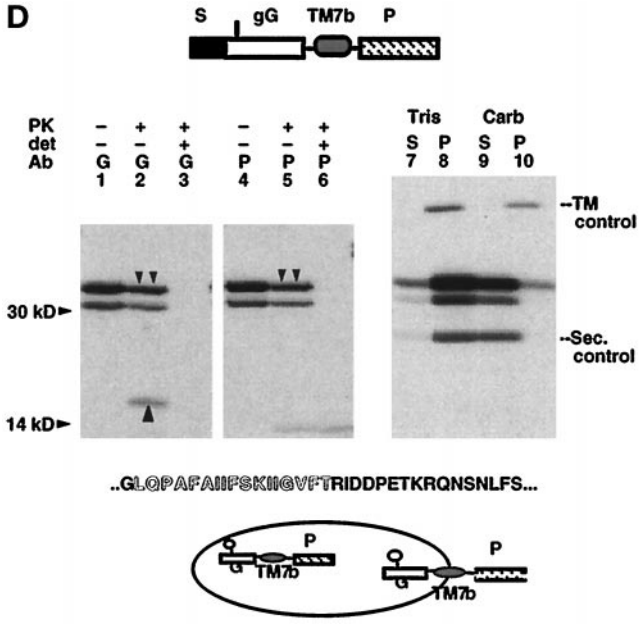

Figure 2D.

tion in only a subset of chains and was unable to efficiently integrate into the lipid bilayer. This was not entirely unexpected, because both the length (17 residues) and hydrophobicity of TM7b (free energy of transfer into the bilayer, 21.2 kcal/mol) are at the lower limits of values expected for traditional membrane-spanning segments (Engelman *et al.*, 1986). However, when we examined a longer version of TM7b encoding 19 residues (N721-R749), the ST activity was not improved (our unpublished observations), suggesting that additional structural features within the hydrophobic segment might contribute to its inefficient ST activity (see Figure 7).

These experiments suggest that the efficient signal sequence activity of TM7 together with the inefficient ST activity of TM7b might direct the nascent polypeptide chain into either of two different TM orientations. In chains where TM7b failed to terminate translocation, TM7 would likely form a single membrane-spanning segment as predicted by conventional topological models. Alternatively, if TM7b terminated translocation, both TM7a and TM7b might potentially span the membrane. It is interesting from a thermodynamic viewpoint that if TM7 interacted independently with the lipid bilayer, the free energy of transfer into the bilayer for two helices formed by TM7a and TM7b would confer a slightly lower free energy than if TM7 spanned the membrane as a single TM helix of 21 residues as originally predicted (42.3 vs. 35.2 kcal/mol, respectively [Engelman *et al.*, 1986]).

TM8 Directs Two Different Membrane-spanning Orientations

One consequence of TM7 adapting two different topological orientations (e.g. single or double spanning) is that downstream topogenic sequences would be presented to the ER membrane in very different contexts. For example, if TM7b terminated translocation, then TM8 would likely emerge from the ribosome in contact with cytosol (Liao *et al.*, 1997). In chains where TM7b failed to terminate translocation, however, TM8 would emerge from the ribosome on an actively translocating chain (presumably moving through the Sec61 translocation channel [Borel and Simon, 1996; Laird and High, 1997] and shielded from the cytosol by the ribosome-membrane junction [Crowley *et al.*, 1993, 1994]). We therefore tested the topogenic behavior of TM8 using two chimeric proteins that mimic these potential presentations of TM8 to the ER by TM7a/b.

As shown in Figure 3A, when TM8 was synthesized as part of an actively translocating chain (plasmid S.gG.TM8.P), it efficiently terminated translocation and integrated into the ER membrane in a type I orientation. Thus TM8 exhibited all the features of a bona fide ST sequence, consistent with its expected role in directing conventional MDR1-Pgp topology. In contrast, when TM8 emerged from the ribosome into the cytosol (plasmid TM8.P), it functioned as an efficient C-*trans* (type II) signal anchor sequence, actively translocating its C-terminal flanking residues and integrating into the membrane in a type II orientation (Figure 3B). Of note, the type II topology of TM8 shown here was identical to the topology observed for murine Pgp-TM8 in *E. coli* (Beja and Bibi, 1995).

The ability of TM8 to direct two different membrane-spanning orientations is not without precedent, because ST sequences have previously been shown to exhibit membrane targeting and translocation activity (Mize *et al.*, 1986). In addition, signal anchor sequences may also function as ST sequences and span the membrane in different orientations (Wessels and Spiess, 1988). The unexpected aspect of these findings is that the translocation specificity of TM8 was precisely the opposite of that predicted if TM8 spanned the membrane solely in the conventional (type I) topology. In this regard, TM7a and TM8 could be viewed as directly competitive with one another, each trying to orient in the ER membrane in a type II topology, not unlike previously described "topologically frustrated" proteins (Gafvelin and von Heijne, 1994). Furthermore, TM7 and TM8 translocation activities are particularly striking when compared with corresponding N-terminal topogenic determinants, TM1 and TM2. In contrast to TM7, TM1 has been previously shown to direct translocation of its C-terminal flanking sequences and to span the membrane as a single TM segment (Skach and Lingappa, 1993). Moreover, when

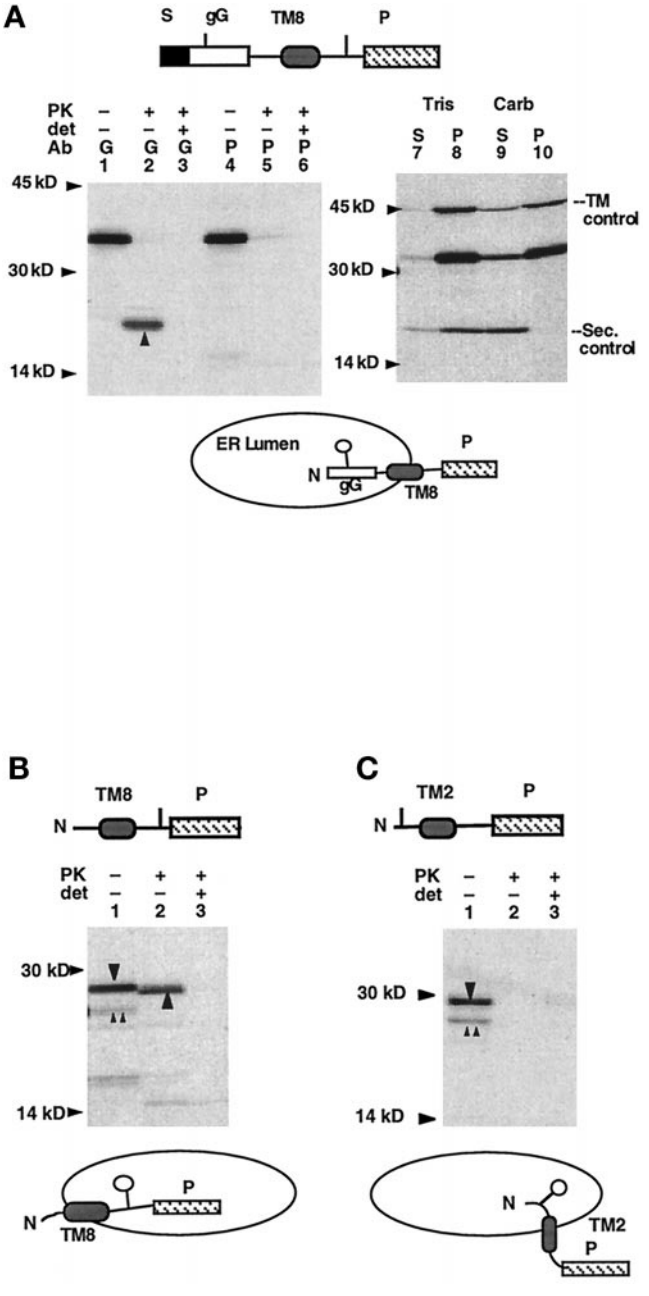

Figure 3. TM8 topology is dependent on its mode of presentation to the ER membrane. (A) Topology of polypeptides generated from plasmid S.gG.TM8.P was determined as in Figure 2. Upward arrow (lane 2) indicates the globin-protected fragment generated by PK digestion, demonstrating a type I topology for these chains (diagrammed beneath the autoradiogram). (B and C) PK digestion of polypeptides generated from plasmids TM8.P and TM2.P. Upward double arrows and downward arrow indicate full-length unglycosylated and glycosylated chains, respectively (lane 1). Upward arrow indicates PK-protected fragment (lane 2). Potential glycosylation sites are indicated in by short vertical lines, and used glycosylation sites are indicated below by the open circles.

examined in the same context as TM8, TM2 directed translocation of N-terminus, rather than C-terminus, flanking sequences and spanned the membrane in a type I topology (Figure 3C). Thus TM1 and TM2 exhibit complementary translocation specificities that cooperate to ensure a uniform N-terminus topology, whereas TM7 and TM8 encode conflicting topogenic information potentially capable of generating two alternate TM orientations.

TM7b and TM8 Generate Topological Heterogeneity in the ER Membrane

Based on the topogenic properties of TM7a, TM7b, and TM8, we predict that during MDR1-Pgp biogenesis, signal sequence activity of TM7a reinitiates translocation of the nascent chain. If translocation were not terminated by TM7b, then TM7 and TM8 would each span the membrane in their proposed, conventional orientations. Alternatively, if TM7b terminated translocation, then signal sequence activity of TM8 would initiate translocation of its own C-terminal flanking residues and span the membrane in an unconventional type II orientation. A key prediction of this model is that distinct topogenic events directed by TM7b (translocation termination) and TM8 (translocation initiation) should be integrally coupled to one another. We tested this prediction first, by examining whether TM7b and TM8 together were sufficient to generate topological heterogeneity; second, by confirming that the fate of TM8 was directly linked to that of TM7b; and third, by identifying structural features responsible for this unusual topogenic behavior.

To examine interactions between TM7b and TM8, MDR1-Pgp residues G723-R817 (encoding TM7b together with TM8) were engineering into the chimeric protein S.gG.TM7b-8.P, and topology of resulting chains was examined in microinjected XOs. These chains encode two N-linked glycosylation consensus sites, one located within the gG passenger domain and the other located within TM8 C-terminal flanking residues as diagrammed in Figure 4. Before PK digestion, two full-length bands migrating at 38 and 41 kDa were observed. These species represent chains containing one (Figure 4, upward arrows) or two (Figure 4, downward arrows) N-linked core carbohydrate groups (Figure 4, lanes 1 and 4). Glycosylation status was verified by digestion with endoglycosidase H and comparison of cell-free translation products synthesized in the presence and absence of membranes (our unpublished observations). Protease digestion confirmed that these polypeptides represent two distinct cohorts of chains with different TM topologies. Singly glycosylated chains (60% of total products) were completely (>95%) accessible to PK digestion and yielded a major, protease-protected 23-kDa globin-reactive

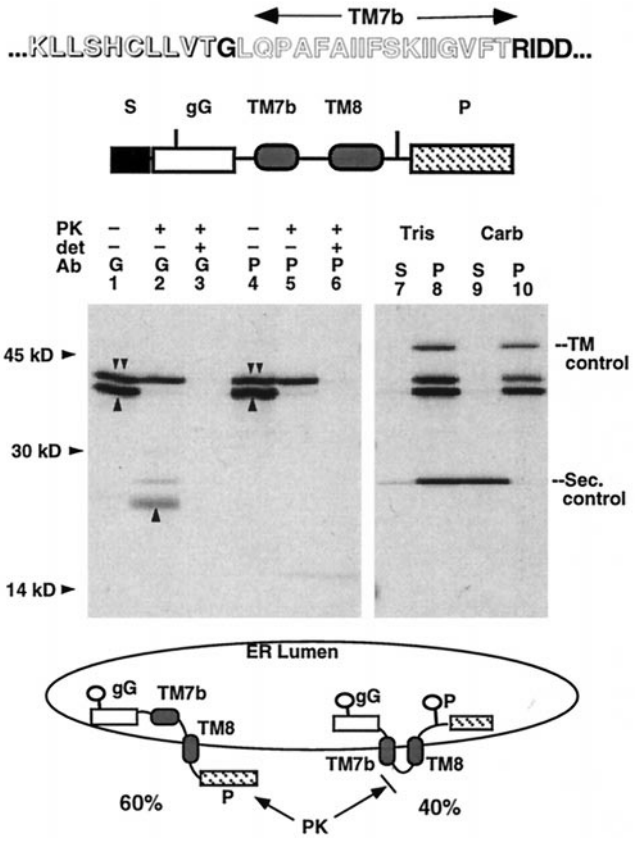

Figure 4. TM7b and TM8 direct two distinct TM orientations for a single population of nascent chains. Oocyte homogenates containing polypeptides from plasmid S.gG.TM7b-8.P were subject to PK digestion (lanes 1–6) or carbonate extraction (lanes 7–10) and immunoprecipitated as described in Figure 2. Upward arrows identify singly glycosylated full-length chains (lanes 1 and 4). Downward double arrows indicate doubly glycosylated full-length chains (lanes 1, 2, 4, and 5) After PK digestion, all singly glycosylated chains are digested, yielding an N-terminal globin-reactive fragment (lane 2, upward arrow), whereas double-glycosylated chains are fully protected. All full-length chains are fully integrated into the bilayer (lanes 7–10). Alternate topological isoforms of these chains are indicated beneath the autoradiograms. The ratios of single-spanning chains versus double-spanning chains were 60 and 40%, respectively. Potential glycosylation sites are indicated as vertical lines, and used sites are indicated as open circles. The sequence of pertinent residues of TM7b and TM8 is indicated in Figure 1.

fragment in the absence of detergent (lane 2, upward arrow). Thus they spanned the membrane in a type I orientation similar to that observed for S.gG.TM7b.P chains (Figure 1C). The protected fragment of S.gG.TM7b-8.P chains, however, was significantly larger than the fragment observed for chains containing only TM7b, 23 versus 17 kDa, respectively (compare Figures 4 and 2D). Thus PK digestion of S.gG.TM7b-8.P must have occurred C-terminal to TM8 rather than C-terminal to TM7b, strongly suggesting that in these chains TM7b failed to terminate translocation and TM8, rather than TM7b, spanned the membrane (diagrammed in Figure 4).

In contrast to singly glycosylated chains, doubly glycosylated chains (40% of total products) were completely (>95%) protected from PK digestion. These polypeptides, therefore, were either secretory in nature, or alternatively, they spanned the membrane with both the globin- and prolactin-derived passenger domains residing in the ER lumen. Carbonate extraction experiments indicated that all chains were fully integrated into the bilayer, a result that could not be explained if chains were lumenal or peripherally associated with the membrane (Figure 4, lanes 7–10). Because both N- and C-terminal domains were glycosylated, TM7b and TM8 must each span the membrane with their N and C termini, respectively, in the ER lumen. In this orientation, the connecting peptide segment between TM7b and TM8 would reside in the cytosol. However, given the limited size of this peptide loop (13 residues), it is not surprising that it would be inaccessible to PK digestion because of steric constraints (Skach *et al.*, 1994). The topology of these chains therefore indicates that translocation termination by TM7b results in translocation reinitiation by the type II signal anchor activity of TM8. The inefficient ST activity of TM7b, coupled together with the signal anchor activity of TM8, therefore appears to be sufficient to generate topological heterogeneity previously observed for MDR1-Pgp.

Although the orientation of TM7b and TM8 in doubly spanning chains in Figure 4 is precisely the orientation reported by Beja and Bibi (1995) for murine Pgp expressed in *E. coli*, it differs from the topology previously proposed by us and Zhang *et al.* (1996), in which it was assumed that TM7 spanned the membrane as a single TM segment (Zhang and Ling, 1991; Skach *et al.*, 1993). This led to the previous conclusion that TM8 (along with TM7 C-terminal flanking residues) was oriented in the ER lumen, a result consistent with the lack of PK accessibility of the short cytosolic peptide segment connecting TM7b and TM8. Given the topological specificities of TM7a, TM7b, and TM8 demonstrated here, our previous data (as well as those of Zhang *et al.*, 1996) are entirely consistent with the topology reported by Beja and Bibi (1995). However, it should be noted that the cooperative topogenic behavior of TM7b and TM8 is such that only a subset of chains, slightly less than half, exhibit this unconventional topology. The remainder of chains appear to adopt a conventional topology consistent with epitope insertion and cysteine labeling studies reported by Loo and Clarke (1995) and Kast *et al.* (1996). The two topological models for TM7a/b and TM8 derived from these studies are shown in Figure 5.

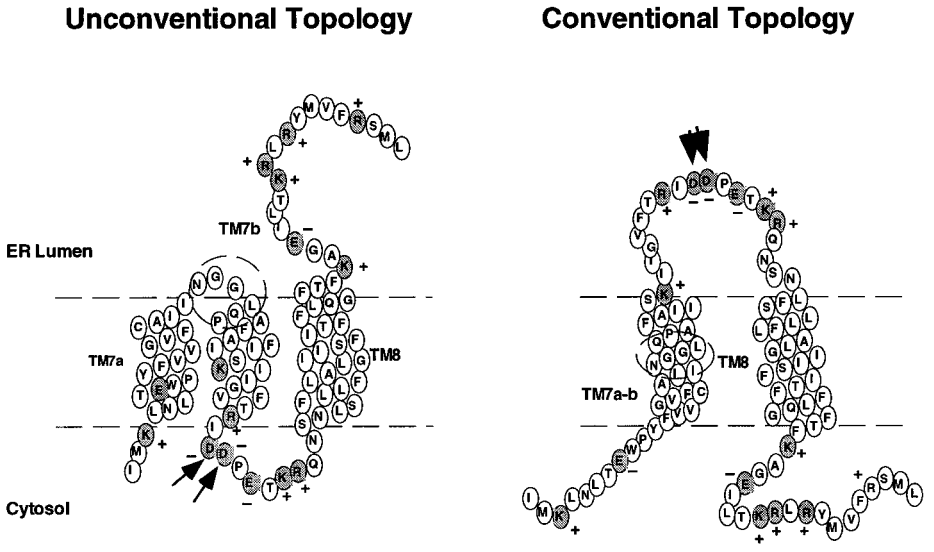

Figure 5. Conventional and unconventional topologies of TM7a/b-TM8 in the ER membrane. Residues within predicted TM segments are indicated. Charged residues within flanking regions are shaded. Boundaries of TM segments are estimated based on the lowest free energy of transfer for partitioning the helix into the lipid bilayer and do not take into account potential interactions with adjacent helices that may shift these boundaries. Dashed circle indicates position of peptide connecting TM7a and TM7b. Arrows indicate positions of residues Asp-743 and Asp-744.

Pleiotropic Structural Information Directs MDR1-Pgp Topological Heterogeneity

To better understand the structural information responsible for directing TM7a, TM7b and TM8 topology, we engineered a series of mutations within TM7a/b and its flanking residues. We reasoned that if TM7 formed two TM segments, then the peptide segment NGG(LQP) between TM7a and TM7b would likely form a tight β turn at the membrane surface (Figure 5), consistent with the high frequency of NGG residues observed at positions +1, +2, and +3 of naturally occurring β turns (Reithmeier and Deber, 1992). Residues N721-P726 (NGGLQP) were therefore replaced with residues MVT in the construct TM7(ΔNGGLQP)a/b.P (Figure 1). As shown in Figure 6A, chains generated from plasmid TM7a/b.P were predominantly oriented in a double-spanning topology in which the P reporter resided in the cytosol (lanes 1–3), consistent with previous studies (Skach *et al.*, 1993). However, the ΔNGGLQP mutation resulted in >50% of chains adapting a single-spanning topology in which the P reporter was translocated into the ER lumen (Figure 6A, lanes 4–6). This mutation had no effect on the ability of TM7 to integrate chains into the membrane, because both WT TM7a/b (our unpublished observations) and TM7(ΔNGGLQP) (Figure 6A, lanes 7–10) were resistant to carbonate extraction. Importantly, deletion of residues NGGLQP from chains containing TM7a/b and TM8 (plasmid TM7a/b[ΔNGGLQP]-8.P) resulted in >90% of chains adapting the conventional topology (Figure 6B, compare lanes 1–3 with 4–10). These results confirm that the NGGLQP peptide loop contributes to MDR1-Pgp topogenic information and provide additional evidence that the TM orientation of TM8 is tightly linked to the topological fate of TM7a/b.

To determine whether the short hydrophobic segment of TM7b might interfere with its ability to terminate translocation and form a stable TM helix, residues GLQP were deleted from TM7b, and the gG passenger domain was fused directly to residue A727 in the plasmid S.gG.TM7b*.P. As shown in Figure 7, this construct encodes 14 residues from the hydrophobic core of TM7b immediately downstream from residues LLSHCLLVT contributed by the globin passenger domain, thus extending the TM7b hydrophobic core to >20 residues in length. Nearly 100% of polypeptides generated from plasmid S.gG.TM7b*.P achieved a type I TM orientation and were capable of integrating into the lipid bilayer (Figure 7A). Furthermore, this increase in TM7b ST activity also altered TM8 topology, as shown by an increased fraction of doubly spanning, protease-protected chains generated from plasmid S.gG.TM7b*-8.P (40% for WT TM7b [Figure 4] compared with 70% for TM7b* [Figure 7B]). Although modest, this increase in the fraction of double-spanning S.gG.TM7b*-8.P chains was significant and consistent in repeated parallel experiments. It should be noted that the hydrophobic residues contributed by the gG passenger are identical in S.gG.TM7b.P and S.gG.TM7b*.P constructs. The only difference between these constructs was the presence or absence of residues GLQP at the N terminus (i.e. fusion site) of TM7b, suggesting that these residues might play a role in determining TM7b ST activity.

Because basic residues in C-terminal flanking sequences are known to provide important information for ST activity (Kuroiwa *et al.*, 1991), we also tested whether mutating residues D743 and D744 to arginine (thus generating a net C-terminal charge of +4 for TM7b; see Figure 5) would alter topology of TM7b and/or TM8. As shown in Figure 8A, the DD→RR

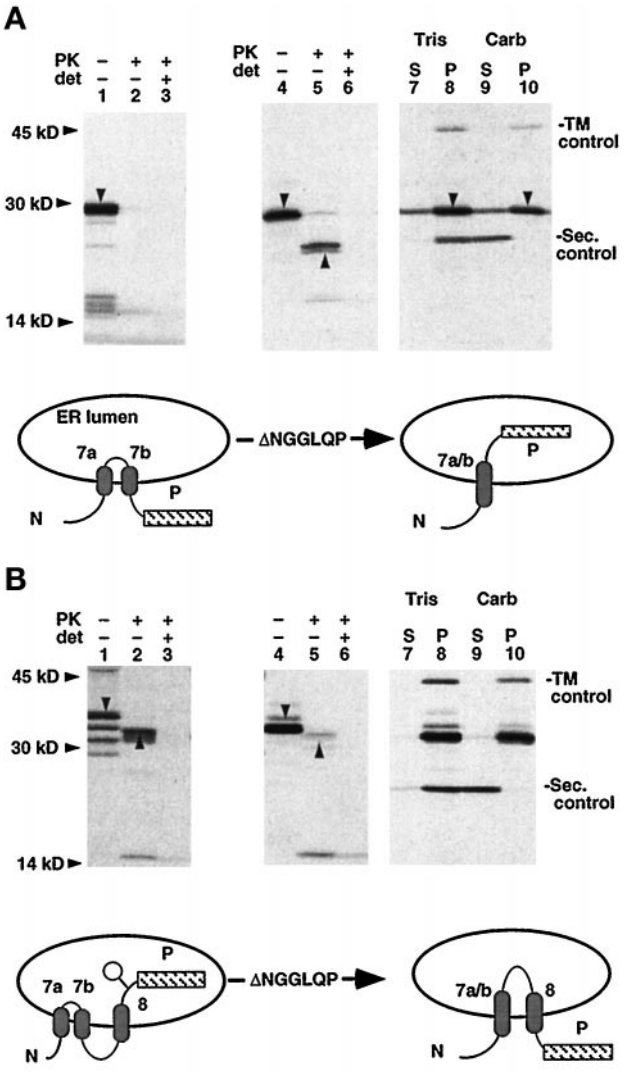

Figure 6. Mutating residues NGGLQP between TM7a and TM7b shift chains toward conventional topology. PK digestion and carbonate extraction of polypeptides containing native (lanes 1–3) or ΔNGGLQP (lanes 4–10) from plasmids TM7a/b.P (A) or TM7a/b-8.P (B). Downward arrows indicate full-length chains, whereas upward arrows indicate protease-protected, P-reactive fragments. Topology of chains relative to the ER membrane is indicated. In B, downward arrows (lanes 1 and 4) indicate full-length glycosylated polypeptides. Additional bands in lane 1 represent unglycosylated polypeptides and cleavage products. The small 15-kDa band (lanes 2 and 5) represents <10% of total chains and is also partially resistant to digestion in the presence of detergent and therefore likely represents a residual fragment of the P reporter.

mutation (plasmid S.gG.TM7b(DD/RR).P) increased TM7b ST activity from 41% and resulted in 70% of chains achieving a TM topology. This increase in TM7b ST activity also shifted TM8 toward a type II orientation in the construct S.gG.TM7b(DD/RR)-8.P (Figure 8B). Ninety-four percent of these latter chains were doubly spanning and protected from protease digestion relative to 41% of WT. Finally, when the DD→RR mutations were engineered into plasmid TM7a/b(DD/RR)-8.P, there was a corresponding increase in both glycosylation efficiency (92% of chains) and in protease protection of the P reporter, confirming a shift in TM8 toward the type II, unconventional topology (compare Figure 8C with WT chains in Figure 6B).

These results identify three independent structural features that contribute to the topogenic behavior of TM7a/b and TM8 and likely play a role in establishing TM7a/b and TM8 topology: 1) the presence of a probable β turn between TM7a and TM7b, 2) the length of the TM7b hydrophobic core, and 3) basic residues flanking the C-terminus of TM7b. Importantly, these results also demonstrate that maneuvers that influenced the inefficient ST activity of TM7b as defined in a simple chimera all conferred a corresponding and predictable shift in the topological outcome of TM8.

Mutations in TM7a/b Confer Expected Topological Changes to Full-Length Pgp

Our results indicate that topogenic information encoded within TM7a/b and TM8 directs the local topology of MDR1-Pgp through a series of definable translocation initiation and termination events. To test whether this topological heterogeneity was also present in full-length MDR1-Pgp and not simply an artifact of our truncated chimeras, we inserted the P reporter at residues R817-L814 in full-length MDR1-Pgp or polypeptide chains encoding the complete C-terminal half of MDR1-Pgp (Figure 9). These epitope-tagged proteins were then expressed in XOs, and the topology of the P reporter was determined by PK digestion and immunoprecipitation. PK digestion of WT full-length as well as C-terminal constructs in ER-derived oocyte microsomes generated a protease-protected, P-reactive fragment of ~40 kDa (Figure 9, lanes 1–3). The size of this fragment corresponded to digestion of MDR1-Pgp at the N-terminal boundary of TM7a and the C-terminal boundary of TM10, consistent with previous studies of full-length native MDR1-Pgp expressed in rabbit reticulocyte lysate (Skach *et al.*, 1993). Based on the methionine distribution and PK protection from several experiments, slightly less than half of these chains exhibited the unconventional topology. We then examined the topology of full-length epitope-tagged MDR1-Pgp proteins containing engineered mutations in TM7 and TM8 flanking residues. As predicted from our chimeric studies, the DD→RR mutation shifted TM8 in nearly all chains into the unconventional topology (Figure 9, lanes 4–6). Surprisingly, however, the ΔNGGLQP mutation had little effect on topology of full-length or C-terminal-half chains (Figure 9, lanes 7–9), suggesting that in

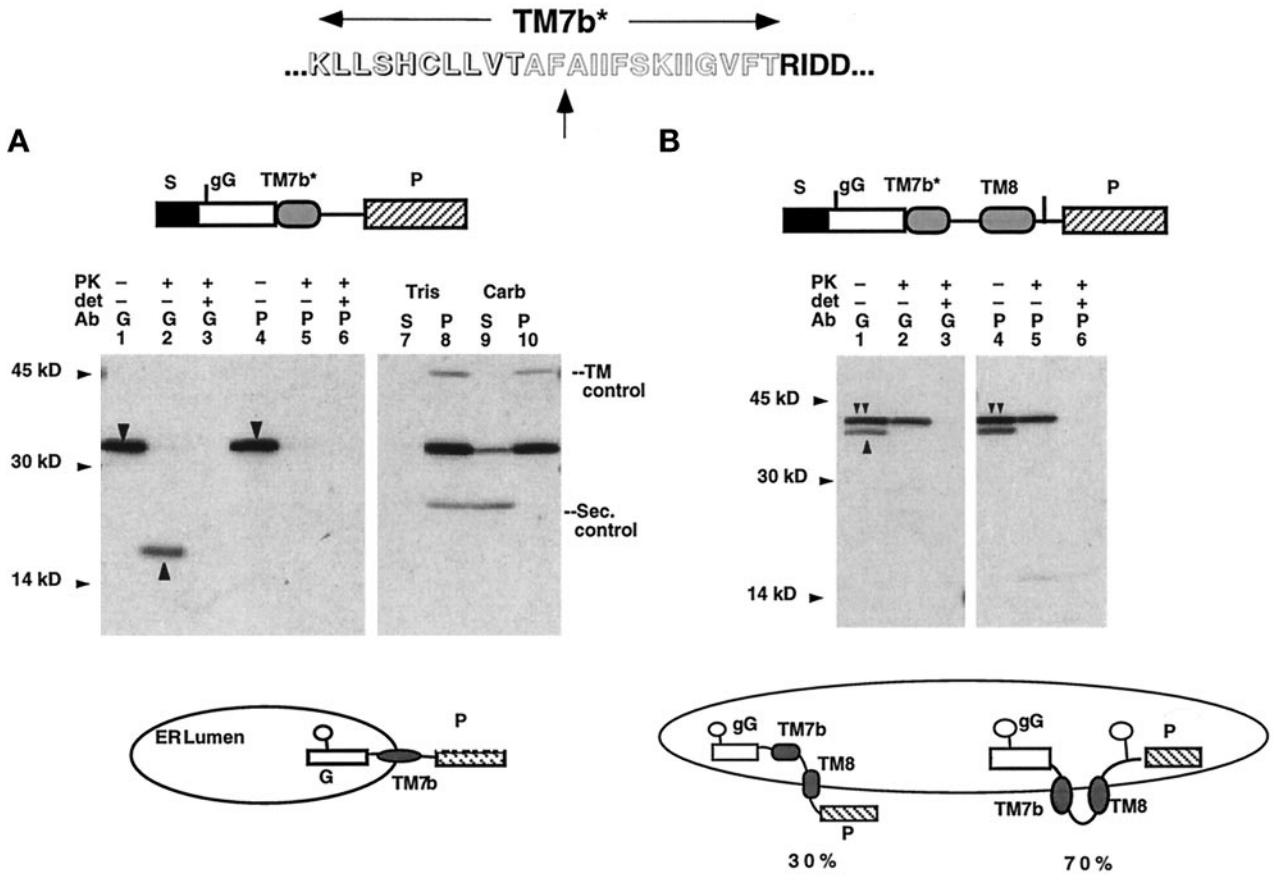

Figure 7. Increasing TM7b ST activity shifts TM8 toward the unconventional topology. Topology of polypeptides from plasmids S.gG.TM7b*.P (A) and S.gG.TM7b*-8.P (B). (A) Downward and upward arrows indicate full-length and PK-protected polypeptides, respectively. The uniform topology of chains is diagrammed. (B) Double and single arrows indicate double- and single-spanning chains, respectively. Topology of these two cohorts of chains is indicated. PK digestion of polypeptides yielded a 23-kDa, globin-reactive fragment in lane 2, which was clearly visible on longer exposure of the autoradiogram (our unpublished observations).

the context of additional topogenic information elsewhere within MDR1-Pgp, the NGGLQP sequence played a relatively minor role in directing MDR1-Pgp topology. Finally when the TM7b and its C-terminal flanking residues (residues K734-S752) were deleted, essentially all chains exhibited the conventional topology, with the P reporter located solely in the cytosol.

DISCUSSION

In this study we identify three distinct native topogenic determinants involved in establishing the TM topology of the MDR1-Pgp C-terminal hydrophobic domain. Our results indicate that these determinants, TM7a, TM7b, and TM8, encode information that is sufficient to direct two alternate topological structures at the ER membrane through a series of definable translocation events. During this process competitive C-*trans* (type II) signal sequence activities encoded within TM7a and TM8 are directly coupled via the inefficient ST activity of TM7b. From the behavior of these determinants, we propose a model to describe the early translocation events that direct topology of this region of the nascent MDR1-Pgp chain (Figure 10). During MDR1 biogenesis, as TM7a emerges from the ribosome, it reinitiates translocation of the nascent chain into the ER lumen. As translation proceeds, TM7b subsequently terminates translocation, but only in a subset of chains. For the remaining chains, translocation continues coincident with polypeptide synthesis. Topogenic information encoded within TM7b therefore appears to play a critical role in determining whether TM7a/b will span the membrane once or twice and hence whether TM8 emerges from the ribosome into an actively gated translocation channel or into the cytosol. When TM7b fails to terminate translocation, TM8 functions as an ST sequence and spans the membrane in its predicted type I orientation. When TM7b terminates translocation, however, the

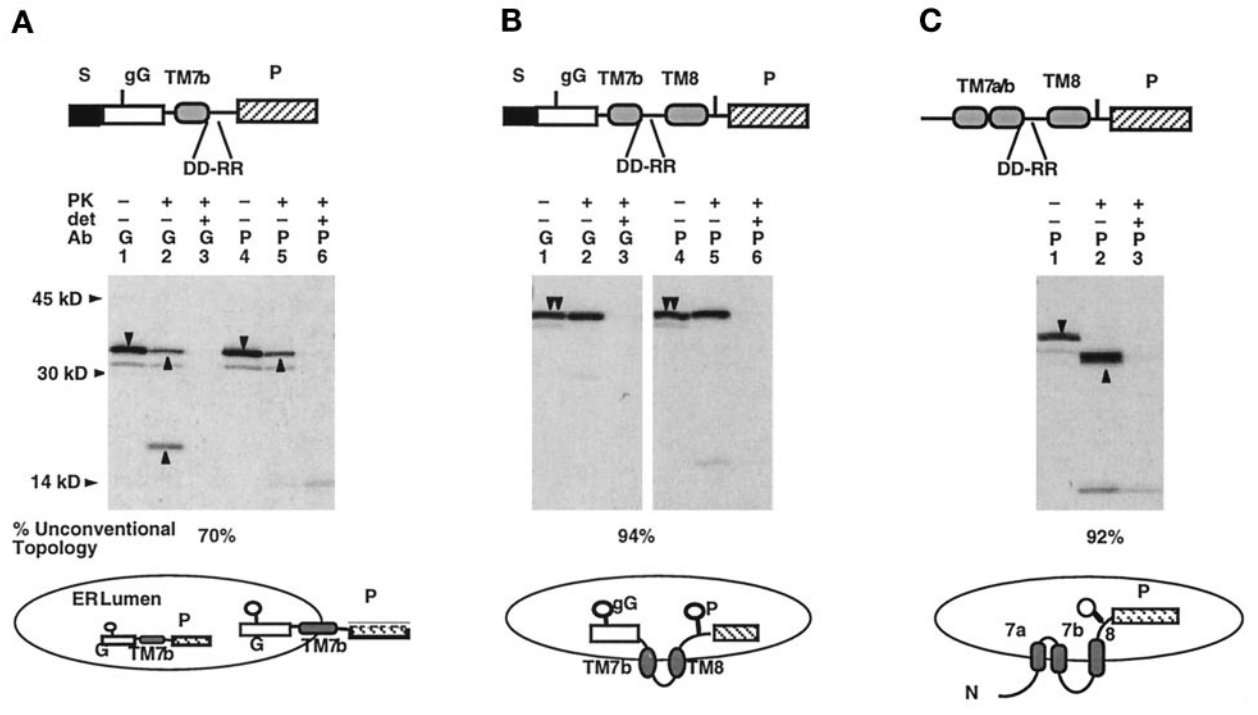

Figure 8. Effect of mutations D743R and D744R on TM7b ST activity and TM8 topology. Topology of polypeptides generated from plasmids S.gG.TM7b(DD/RR).P (A), S.gG.TM7b(DD/RR)-8.P (B), and TM7a/b(DD/RR).P (C) was determined as described in Figure 2. Downward and upward arrows indicate full-length chains and PK-protected fragments, respectively. Topology of resulting chains is diagrammed, and the percent of polypeptides in the unconventional Pgp topology is indicated.

type II signal anchor activity of TM8 reinitiates translocation of TM8 C-terminal flanking residues, directing TM8 into an unconventional type II topology and localizing the TM8-TM9 peptide within the ER lumen. The behavior of these topogenic determinants thus provides a mechanism, or sequence of events, by which a newly synthesized polytopic protein may be directed into either of two alternate TM topologies. In addition, the C-*trans* (type II) signal anchor activity of TM8, in actively translocating the TM8–9 peptide loop into the ER lumen, now provides an explanation for previous topological studies that found this peptide loop to reside in an extracytosolic orientation.

Recent studies have indicated that, as with secretory and bitopic proteins, translocation of polytopic proteins is mediated by the Sec61 translocon channel (Laird and High, 1997; Mothes *et al.*, 1997). Furthermore, during ST-mediated translocation termination, the translocon channel is gated closed at the ER lumen (Hamman *et al.*, 1998), and the nascent chain rapidly becomes exposed to the cytosol (Skach and Lingappa, 1994; Liao *et al.*, 1997). Based on these observations, our model proposes that when TM7b terminates translocation, TM8 emerges from the ribosome in a cytosolically accessible orientation. Given the short connecting peptide loop between TM7b and TM8 (13 residues), however, it is likely that TM8 is actually located between the ribosome exit site and the translocon proper (Blobel and Sabatini, 1970; Liao *et al.*, 1997). An important aspect of this process, therefore, is precisely how the weak ST activity of TM7b interacts with TM8 to influence the gated state of the translocon channel (Liao *et al.*, 1997). It is possible that TM7b simply fails to terminate translocation in a subset of chains and that, for these chains, the translocon remains open until it is subsequently closed by TM8. Alternatively, TM7b may effectively terminate translocation but may be unable to maintain chains in a stable TM conformation, thus functioning analogously to a pause transfer sequence and allowing translocation to restart (Chuck and Lingappa, 1992; Hedge and Lingappa, 1996). In this latter case TM7b, together with its C-terminal flanking residues and TM8, might therefore provide a potential mechanism for topological regulation, as has been proposed for other pause transfer-containing proteins (Lopez *et al.*, 1990; Fisher *et al.*, 1997).

It is important to note that although TM7b appears to be a primary determinant responsible for generating MDR1-Pgp topological heterogeneity, TM8 and its flanking residues are also involved. For example, if TM8 influenced whether TM7b was effectively able to terminate translocation and/or close the translocon gate, then TM8 would also influence the final topology

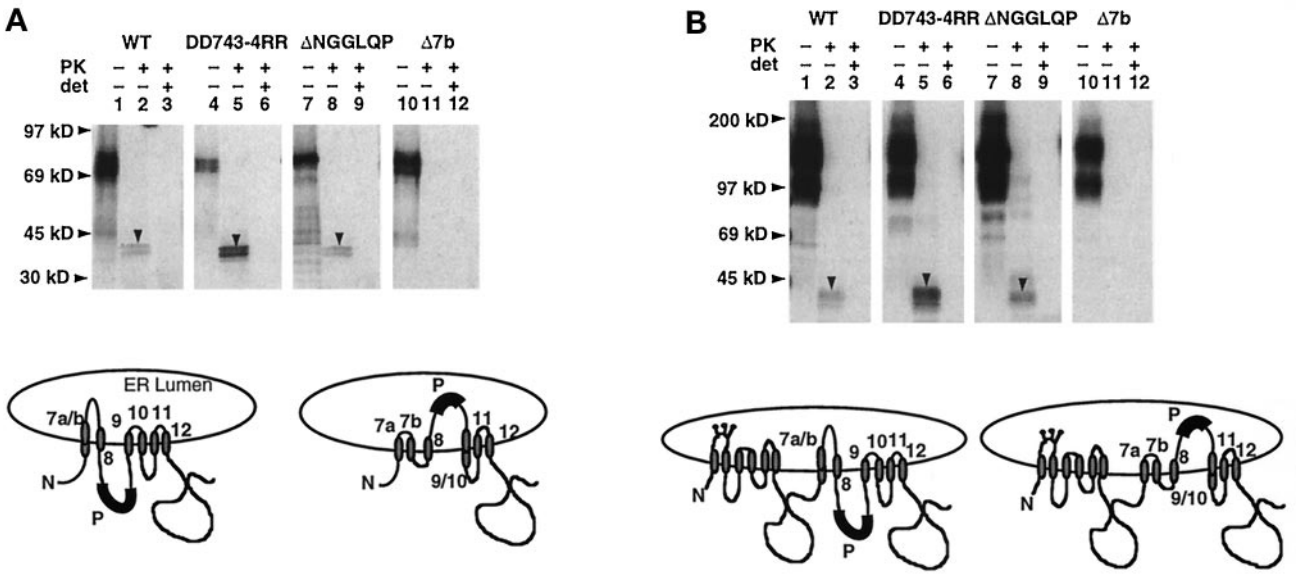

Figure 9. Topology of epitope-tagged full-length Pgp. Proteins encoding the C-terminal half (A) or full-length (B) MDR1-Pgp tagged with the P reporter between TM8 and TM9 was expressed in oocytes and subjected to PK digestion as in Figure 2. Polypeptides migrated at 73 kDa (for C-terminal constructs) and 150 kDa (for full-length MDR1-Pgp). The smear of full-length protein was likely due in part to immunoprecipitation artifact. Protease-protected P-reactive fragments generated by protease digestion are indicated by downward arrows.

of TM7b. Such a mechanism appears to occur because in MDR1-Pgp chains truncated before TM8, TM7a/b exhibited primarily an unconventional (double-spanning) topology, whereas after synthesis of TM8, TM7a/b was nearly evenly divided between conventional (single-spanning) and unconventional (double-spanning) topologies (Skach and Lingappa, 1993) (Figure 6). Thus in the context of TM7a/b, the presence of TM8 decreases the tendency of TM7b to terminate translocation, suggesting that complex interactions between TM7a–TM7b–TM8 and the translocation machinery ultimately regulate the topological fate of this peptide region.

In several aspects the topological heterogeneity observed for TM7a/b–TM8 is strikingly similar to the "topologic frustration" previously reported for experimentally engineered *E. coli* proteins (Gafvelin and von Heijne, 1994). First, the translocation specificities of TM7a and TM8 are in direct competition with one another; both determinants act to translocate their C-terminal flanking sequences. Second, the distribution of basic residues are quite similar for either topological orientation (Figure 5). Such conflicting and/or ambiguous topogenic information was critical in engineering artificial "topologically frustrated" prokaryotic proteins. In contrast to previous studies, however, our data identify native topogenic determinants whose behavior is influenced by pleiotropic structural features that include 1) the hydrophobic region of TM7b, 2) a potential tight β-turn located between TM7a and TM7b, and 3) the distribution of TM7b C-terminal charged flanking residues. Because these determinants reside in a native eukaryotic polytopic protein, we prefer the term topological heterogeneity to describe this phenomenon. Mutations that altered these features all shifted the ratio of chains found in the conventional versus unconventional topology in a predictable manner. Moreover, each of these mutations (e.g., D743R/D744R, ΔNGGLQP, and Δ7b) also affected the stability and intracellular trafficking of full-length MDR1-Pgp protein in intact XOs (Bragin and Skach, unpublished observations), suggesting that structural features responsible for topological heterogeneity of MDR1-Pgp also contribute important information for protein maturation in cells.

How can the results reported here be reconciled with previous studies supporting a conventional 12-spanning topology for Pgp (Yoshimura *et al.*, 1989; Georges *et al.*, 1993; Schinkel *et al.*, 1993; Loo and Clarke, 1995; Kast *et al.*, 1996)? Although the current study provides insight into specific steps in the biogenesis of nascent Pgp chains as they are synthesized at the ER membrane, it is addressing fundamentally different questions than studies examining mature protein topology at the plasma membrane. In this regard, it does not address whether the unconventional MDR1-Pgp isoform functions in conferring drug resistance. It is conceivable that Pgp could exhibit different topologies at different cellular locations or stages of biosynthesis. The unconventional topological isoform may simply comprise a cohort of misfolded chains that fails to mature and exit the ER or,

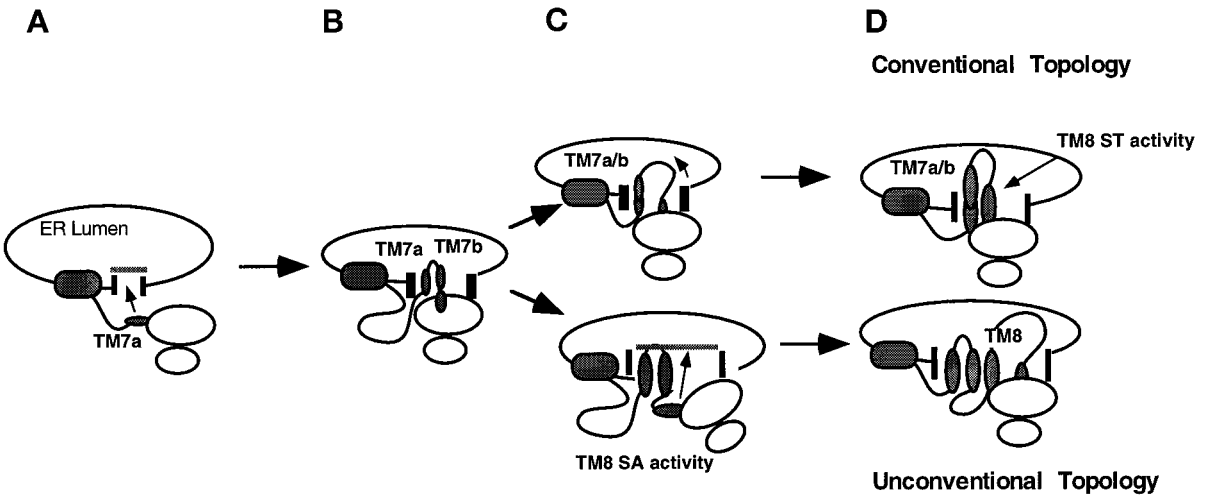

Figure 10. Schematic model for generating topological heterogeneity in the ER membrane. Depicted are translocation events and topological intermediates proposed to participate in MDR1-Pgp topogenesis. After translocation reinitiation by TM7a (A), TM7b and TM8 emerge from the ribosome into the translocation channel (B) where the nascent chain faces two topological fates. In one cohort of chains TM7b fails to terminate translocation (C), and the chain continues to move into the ER lumen until translocation is terminated by ST activity of TM8. In the second cohort of chains, translocation is terminated by TM7b and subsequently reinitiated by the C-*trans* (type II) signal sequence activity of TM8. Large and small shaded ovals represent the Pgp N-terminal hydrophobic domain and individual TM segments, respectively. Translocation machinery is indicated by vertical bars. The diagram is meant only to describe the temporal sequence of specific translocation events. The precise nature of interactions among the ribosome, translocon, TM segments, and lipid bilayer is unknown.

alternatively, a transient folding intermediate that acquires a conventional topology as downstream TM segments are synthesized and assembled. This seems unlikely, however, for two reasons. First, newly synthesized Pgp is efficiently trafficked out of the ER and processed by Golgi enzymes (Jensen *et al.*, 1995). Second, immunofluorescence analyses of native Pgp in intact mammalian cells has suggested that the TM8–9 peptide loop contributes to an extracellular epitope on at least some molecules at the plasma membrane (Poloni *et al.*, 1995; Zhang *et al.*, 1996). An alternate possibility is that distinct topological isoforms of Pgp may perform different functions or even act primarily in different subcellular compartments. Such a phenomenon has been reported for the polytopic protein ductin (Finbow *et al.*, 1994). A third possibility is that different MDR1-Pgp topological isoforms may represent alternate states of a dynamic TM structure analogous to the bacterial translocation components SecA and SecG (Economou and Wickner, 1994; Nishiyama *et al.*, 1996), the Na, K-ATPase (Lutsenko *et al.*, 1995), or the voltage-sensitive channel colicin (Slatin *et al.*, 1994).

Because different expression systems may yield different topological outcomes for a given protein (Hay *et al.*, 1987a,b; Wohlwend *et al.*, 1987; Lopez *et al.*, 1990), it remains possible that the relative efficiency of generating different MDR1-Pgp isoforms might vary between different cell types or even under different environmental conditions. For this reason MDR1-Pgp topogenic determinants were characterized entirely in XOs that process MDR1-Pgp efficiently (Skach, unpublished observations) and that are capable of generating functionally mature Pgp protein (Castillo *et al.*, 1990). Our data indicate that the topogenic activities of TM7a, TM7b, and TM8 in oocytes are entirely consistent with results of previous studies using reconstituted mammalian and prokaryotic expression systems.

Finally, our results suggest that different orientations of TM7a/b-TM8 may influence, and are influenced by, downstream or distant regions of MDR1-Pgp. It is intriguing that, like TM7a/b, TM9–10 comprises a continuous 40-residue hydrophobic region and that residues C-terminal to TM10 are cytosolically accessible even in full-length polypeptides exhibiting unconventional topology (Figure 9). This would suggest that 1) TM9–10, like TM7a/b, might also be able to achieve a single-spanning orientation depending on the topology of TM7a/b-TM8; and 2) the unconventional isoform does not require a change in the topology of TM11–12 or of the C terminus. Alternatively, synthesis of TM9–10 may in some manner influence the final topology of TM7a/b-8. The observation that the ΔNGGLQP mutation had a prominent effect on the topology of small Pgp fragments but had little effect on the topology of full-length MDR1-Pgp protein indicates that other regions of MDR1-Pgp might influence the final topology of TM7a/b and TM8 in the mature protein. Such a phenomenon has been observed during Sec61p topogenesis in yeast (Wilkinson *et al.*, 1996). It is clear from these studies that both local and distant structural

features can ultimately impact polytopic protein topology. Specific translocation events that occur at a particular stage of biogenesis should thus be viewed as representing a relatively early aspect of the entire biosynthetic process and should not be interpreted to unequivocally establish the final topology of functionally mature protein. Rather, these studies should be viewed in the context of unraveling the complex nature of events that must occur during the process of polytopic protein topogenesis. Ultimately, such knowledge will be important in developing models that more accurately explain how these proteins are generated.

ACKNOWLEDGMENTS

We thank Drs. D. Pain and C. Deutsch for helpful comments with the manuscript. This work was supported by National Institutes of Health grants GM53457 and DK51818 and funding from the North American Cystic Fibrosis Foundation.

REFERENCES

Akiyama, Y., Inada, T., Nakamura, Y., and Ito., K. (1990). Sec Y, a multispanning integral membrane protein, contains a potential leader peptidase cleavage site. J. Bacteriol. *172*, 2888–2893.

Audigier, Y., Friedlander, M., and Blobel, G. (1987). Multiple topogenic sequences in bovine opsin. Proc. Natl. Acad. Sci. USA *84*, 5783–5787.

Beja, O., and Bibi, E. (1995). Multidrug resistance protein (Mdr)-alkaline phosphatase hybrids in *Escherichia coli* suggest a major revision in the topology of the C-terminal half of Mdr. J. Biol. Chem. *270*, 12351–12354.

Belin, D., Bost, S., Vassalli, J.-D., and Strub, K. (1996). A two step recognition of signal sequences determines the translocation efficiency of proteins. EMBO J. *15*, 468–478.

Belin, D., Wohlend, A., Schleuning, W.-D., Kruithof, E., and Vassalli, J.-D. (1989). Facultative polypeptide translocation allows a single mRNA to encode the secreted and cytosolic forms of plasminogen activators inhibitor 2. EMBO J. *8*, 3287–3294.

Blobel, G. (1980). Intracellular protein topogenesis. Proc. Natl. Acad. Sci. USA *77*, 1496–1500.

Blobel, G., and Sabatini, D. (1970). Controlled proteolysis of nascent polypeptides in rat liver cell fractions. I. Localization of polypeptides within ribosomes. J. Cell Biol. *45*, 130–145.

Borel, A., and Simon, S. (1996). Biogenesis of polytopic membrane proteins: Membrane segments assemble within translocation channels prior to membrane integration. Cell *85*, 379–389.

Calamia, J., and Manoil, C. (1992). Membrane protein spanning segments as export signals. J. Mol. Biol. *224*, 539–543.

Castillo, G., Vera, J.C., Yang, C.-P.H., Horwitz, S.B., and Rosen, O.M. (1990). Functional expression of murine multidrug resistance in *Xenopus laevis* oocytes. Proc. Natl. Acad. Sci. USA *87*, 4737–4741.

Chen, C.-J., Chin, J.E., Ueda, K., Clark, D.P., Pastan, I., Gottesman, M.M., and Ronninson, I.B. (1986). Internal duplication and homology with bacterial transport proteins in the mdr1 (P-glycoprotein) gene from multidrug resistant human cells. Cell *47*, 381–389.

Chuck, S., and Lingappa, V.R. (1992). Pause transfer: a topogenic sequence in apolipoprotein B mediates stopping and restarting of translocation. Cell *68*, 9–21.

Crowley, K., Liao, S., Worrell, V., Reinhart, G., and Johnson, A. (1994). Secretory proteins move through the endoplasmic reticulum membrane via an aqueous, gated pore. Cell *78*, 461–471.

Crowley, K., Reinhart, G., and Johnson, A. (1993). The signal sequence moves through a ribosomal tunnel into a noncytoplasmic aqueous environment at the ER membrane early in translocation. Cell *73*, 1101–1115.

De Fea, K., Nakahara, D., Calayag, M.C., Yost, C., Mirels, L., Pruisner, S., and Lingappa, V. (1994). Determinants of carboxyl terminal domain translocation during prion protein biogenesis. J. Biol. Chem. *269*, 16810–16820.

Dunlop, J., Jones, P., and Finbow, M. (1995). Membrane insertion and assembly of ductin: a polytopic channel with dual orientations. EMBO J. *14*, 3609–3616.

Economou, A., and Wickner, W. (1994). SecA promotes preprotein translocation by undergoing ATP-driven cycles of membrane insertion and deinsertion. Cell *78*, 835–843.

Engelman, D., Steitz, T., and Goldman, A. (1986). Identifying nonpolar transmembrane helices in amino acid sequences of membrane proteins. Annu. Rev. Biophys. Biophys. Chem. *15*, 321–353.

Finbow, M., Goodwin, S., Meagher, L., Lane, N., Keen, J., Findlay, J., and Kaiser, K. (1994). Evidence that the 16 kDa proteolipid (subunit c) of the vacuolar H(+)-ATPase and ductin from gap junctions are the same polypeptide in *Drosophila* and *Manduca*: molecular cloning of the Vha16k gene from *Drosophila*. J. Cell Sci. *107*, 1817–1824.

Fisher, E., Zhou, M., Mitchell, D., Wu, X., Omura, S., Wang, H., Goldberg, A., and Ginsberg, H. (1997). The degradation of apolipoprotein B100 is mediated by the ubiquitin-proteasome pathway and involves heat shock protein 70. J. Biol. Chem. *272*, 20427–20434.

Friedlander, M., and Blobel, G. (1985). Bovine opsin has more than one signal sequence. Nature *318*, 338–343.

Gafvelin, G., and von Heijne., G. (1994). Topological "frustration" in multispanning *E. coli* inner membrane. Cell *77*, 401–412.

Georges, E., Tsuro, T., and Ling, V. (1993). Topology of P-glycoprotein as determined by epitope mapping of MRK-16 monoclonal antibody. J. Biol. Chem. *268*, 1792–1798.

Gros, P., Croop, J., and Housman, D. (1986). Mammalian multidrug resistance gene: complete cDNA sequence indicates strong homology to bacterial transport proteins. Cell *47*, 371–380.

Hamman, B., Hendershot, L., and Johnson, A. (1998). Bip maintains the permeability of the ER membrane by sealing the lumenal end of the translocon pore before and early in translocation. Cell *92*, 747–758.

Hay, B., Barry, R., Lieberburg, I., Prusiner, S., and Lingappa, V.R. (1987a). Biogenesis and transmembrane orientation of the cellular isoform of the scrapie prion protein. Mol. Cell. Biol. *7*, 914–920.

Hay, B., Prusiner, S., and Lingappa, V.R. (1987b). Evidence for a secretory form of the cellular prion protein. Biochemistry *26*, 8110–8115.

Hedge, K., and Lingappa, V. (1996). Sequence-specific alteration of the ribosome-membrane junction exposes nascent secretory proteins to the cytosol. Cell *85*, 721–732.

Ho, N., Hunt, H., Horton, R., Pullen, J., and Pease, P. (1989). Site-directed mutagenesis by overlap extension using the polymerase chain reaction. Gene *77*, 51–59.

Jensen, T., Loo, M., Pind, S., Williams, D., Goldberg, A., and Riordan, J. (1995). Multiple proteolytic systems, including the proteosome, contribute to CFTR processing. Cell *83*, 129–136.

Johnson, A. (1997). Protein translocation at the ER membrane: a complex process becomes more so. Trends Cell Biol. *7*, 90–94.

Kast, C., Canfield, V., Levenson, R., and Gros, P. (1996). Transmembrane organization of mouse P-glycoprotein determined by epitope insertion and immunofluorescence. J. Biol. Chem. *271*, 9240–9248.

Kuroiwa, T., Sakaguchi, M., Mihara, K., and Omura, T. (1991). Systematic analysis of stop-transfer sequence for microsomal membrane. J. Biol. Chem. *266*, 9251–9255.

Laird, V., and High, S. (1997). Discrete cross-linking products identified during membrane protein biosynthesis. J. Biol. Chem. *271*, 1983–1989.

Liao, S., Lin, J., Do, H., and Johnson, A. (1997). Both luminal and cytosolic gating of the aqueous translocon pore are regulated from inside the ribosome during membrane protein integration. Cell *90*, 31–42.

Lin, J., and Addison, R. (1995). A novel integration signal that is composed of two transmembrane segments is required to integrate the neorospora plasma membrane H+-ATPase into microsomes. J. Biol. Chem. *270*, 6935–6941.

Lipp, J., Flint, N., Haeuptle, M.T., and Dobberstein, B. (1989). Structural requirements for membrane assembly of proteins spanning the membrane several times. J. Cell Biol. *109*, 2013–2022.

Loo, T., and Clarke, D. (1995). Membrane topology of a cysteine-less mutant of human P-glycoprotein. J. Biol. Chem. *270*, 843–848.

Lopez, C.D., Yost, C.S., Prusiner, S.B., Myers, R.M., and Lingappa, V.R. (1990). Unusual topogenic sequence directs prion protein biogenesis. Science *248*, 226–229.

Lu, Y., Xiong, X., Bragin, A., Kamani, K., and Skach, W. (1997). Co- and posttranslational mechanisms direct CFTR N-terminus transmembrane assembly. J. Biol. Chem. *273*, 568–576.

Lutsenko, S., Anderko, R., and Kaplan, J. (1995). Membrane disposition of the M5–M6 hairpin of the Na, K-ATPase a-subunit is ligand dependent. Proc. Natl. Acad. Sci USA *92*, 7936–7940.

Mize, N.K., Andrews, D.W., and Lingappa, V.R. (1986). A stop transfer sequence recognizes receptors for nascent chain translocation across the endoplasmic reticulum membrane. Cell *47*, 711–719.

Mothes, W., Heinrich, S., Graf, R., Nilsson, I., von Heijne, G., Brunner, J., and Rapoport, T. (1997). Molecular mechanism of membrane protein integration into the endoplasmic reticulum. Cell *89*, 523–533.

Nakahara, D., Lingappa, V., and Chuck, S. (1994). Translocational pausing is a common step in the biosynthesis of unconventional integral membrane and secretory proteins. J. Biol. Chem. *269*, 7617–7622.

Nishiyama, K., Suzuki, T., and Tokuda, H. (1996). Inversion of the membrane topology of SecG coupled with SecA-dependent preprotein translocation. Cell *85*, 71–82.

Parks, G., and Lamb, R. (1991). Topology of eukaryotic type II membrane proteins: importance of N-terminal positively charged residues flanking the hydrophobic domain. Cell *64*, 777–787.

Parks, G.D., Hull, D., and Lamb, R.A. (1989). Transposition of domains between the M2 and HN viral membrane proteins results in polypeptides which can adopt more than one membrane orientation. J. Cell Biol. *109*, 2023–2032.

Poloni, F., Romagnoli, G., Cianfriglia, M., and Felici, F. (1995). Isolation of antigenic mimics of MDR1-P-glycoprotein by phage-displayed peptide libraries. Int. J. Cancer *61*, 727–731.

Rapoport, T., Rolls, M., and Jungnickel, B. (1996). Approaching the mechanism of protein transport across the ER membrane. Curr. Opin. Cell Biol. *8*, 499–504.

Reithmeier, R., and Deber, C. (1992). Intrinsic membrane protein structure: principles and predictions. In: The Structure of Biological Membranes, ed. P. Yeagle, Boca Raton, FL: CRC Press, 337–393.

Rothman, R.E., Andrews, D.W., Calayag, M.C., and Lingappa, V.R. (1988). Construction of defined polytopic integral transmembrane proteins. J. Biol. Chem. *263*, 10470–10480.

Schinkel, A., Arceci, R., Smit, J., Wagenaar, E., Baas, F., Dolle, M., Tsururo, T., Mechetner, E., Foninson, I., and Borst, P. (1993). Binding properties of monoclonal antibodies recognizing external epitopes of the human MDR1 P-glycoprotein. Int. J. Cancer *55*, 478–484.

Schmid, S.R., and Spiess, M. (1988). Deletion of the amino-terminal domain of asialoglycoprotein receptor H1 allows cleavage of the internal signal sequence. J. Biol. Chem. *163*, 16886–16891.

Shi, L.-B., Skach, W., Ma, T., and Verkman, A. (1995). Distinct biogenesis mechanisms for water channels MIWC and CHIP28 at the endoplasmic reticulum. Biochemistry *34*, 8250–8256.

Skach, W., Calayag, M.C., and Lingappa, V. (1993). Evidence for an alternate model of human P-glycoprotein structure and biogenesis. J Biol. Chem. *268*, 6903–6908.

Skach, W., and Lingappa, V. (1993). Amino terminus assembly of human P-glycoprotein at the endoplasmic reticulum is directed by cooperative actions of two internal sequences. J. Biol. Chem. *268*, 23552–23561.

Skach, W., and Lingappa, V. (1994). Transmembrane orientation and topogenesis of the 3rd and 4th membrane-spanning regions of human P-glycoprotein (MDR1). Cancer Res. *54*, 3202–3209.

Skach, W., Shi, L.-B., Calayag, M.C., Frigeri, A., Lingappa, V., and Verkman, A. (1994). Biogenesis and transmembrane topology of the CHIP28 water channel in the endoplasmic reticulum. J. Cell Biol. *125*, 803–815.

Slatin, S., Qui, X.-Q., Jakes, K., and Finkelstein, A. (1994). Identification of a translocated protein segment in a voltage-dependent channel. Nature *371*, 158–161.

Wessels, H., and Spiess, M. (1988). Insertion of a multispanning membrane protein occurs sequentially and requires only one signal sequence. Cell *55*, 61–70.

Wilkinson, B., Critchley, A., and Stirling, C. (1996). Determination of the transmembrane topology of yeast Sec61p, an essential component of the endoplasmic reticulum translocation complex. J. Biol. Chem. *271*, 25590–25597.

Wohlwend, A., Belin, D., and Vassalli, J.-D. (1987). Plasminogen activator-specific inhibitors produced by human monocytes/macrophoges. J. Exp. Med. *165*, 320–339.

Xiong, X., Bragin, A., Widdicombe, J., Cohn, J., and Skach, W. (1997). Structural cues involved in ER degradation of G85E and G91R mutant CFTR. J. Clin. Invest. *100*, 1079–1088.

Yoshimura, A., Kuwazuru, Y., Sumizawa, T., Ichikawa, M., Ikeda, S., Uda, T., and Akitama, S. (1989). Cytoplasmic orientation and two-domain structure of the multidrug transporter, P-glycoprotein, demonstrated with sequence-specific antibodies. J. Biol. Chem. *264*, 16282–16291.

Yost, C.S., Lopez, C.D., Prusiner, S.B., Meyers, R.M., and Lingappa, V.R. (1990). Non-hydrophobic extracytoplasmic determinant of stop transfer in the prion protein. Nature *343*, 669–672.

Zhang, J.-T., and Ling, V. (1991). Study of membrane orientation and glycosylated extracellular loops of mouse P-glycoprotein by in vitro translation. J. Biol. Chem. *266*, 18224–18232.

Zhang, M., Wang, G., Shapiro, A., and Zhang, J.-T. (1996). Topological folding and proteolysis profile of P-glycoprotein in membranes of multidrug-resistant cells: implication for drug transport mechanisms. Biochemistry *35*, 9728–9736.